Implementation of the Hertz Contact Model and Its Volumetric Modification on Modelica

Ivan Kosenko Evgeniy Alexandrov
Russian State University of Tourism and Service, Department of Engineering Mechanics
Glavnaya str. 99, Cherkizovo-1, Moscow reg., 141221, Russia

Abstract

The Hertz model of an elastic bodies contact and its volumetric modification are analyzed for the proper implementation on Modelica. Computational algorithms applied aim to accelerate the simulation process and make it more reliable.
The algorithm tracking the surfaces of the bodies which are able to contact was improved using its differential version and showed an accuracy high enough.
Simulation of the Hertz model was accelerated due to use of the differential technique to compute the complete elliptic integrals and due to the replacement of the implicit transcendental equation by the differential one.
To have a reliable model for the simulation of the contact especially in case of the contact spot ellipses of an eccentricity high enough the volumetric modification of Hertz model is introduced. The model showed a reliable behavior and an acceptable accuracy.
Finally an implementation of the ball bearing model as an example of the contact models application is under consideration. The particular bearings being analyzed can have different number of balls and different types of raceways. The bearing models created using the library of classes developed earlier and have an outside look exactly like a mechanical constraints and behave in some degree similar to the revolute joints.
Keywords: Hertz contact model, volumetric approach, ball bearing model

1 Introduction

It is known [1] to compute a force of the elastic bodies interaction at a contact several different approaches are applied: (a) the classical Hertz model [2], (b) the model based on the polygonal approximation of the contacting surfaces [3] applied to cases of the surfaces of a complex shape and implemented on Modelica [4], (c) the volumetric model [1, 5]. In our model we follow the classical Hertz approach, and the normal force computation method is a main topic of our analysis. To handle with the surfaces at the contact we apply an approach mentioned in [4] as variant 2: algebraic constraint surfaces, which we frequently use in our models. For definiteness and simplicity to simulate the tangent contact force one uses a regularized model of the Coulomb friction [6]. This is sufficient enough to simulate the dynamics over time of the machine under simulation lifecycle. May be some additional complications for the friction model, e. g. an account of the lubrication of any type, will be needed.

2 Reduction in Vicinity of Contact

Keeping a frame of the formalism applied previously to simulate a unilateral constraint [6] consider its particular case corresponding to mechanics of contact interaction for two elastic bodies, identified hereafter as *A* and *B*. Their outer surfaces, see Figure 1, being at contact supposed sufficiently regular.

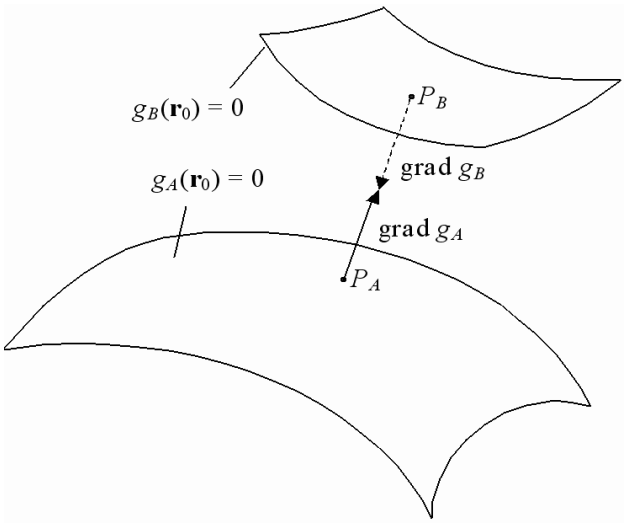

Figure 1: Vicinity of the Contact Area

Applying the same notations as ones used in [6] we

start here by reproducing the system of eight scalar algebraic equations

$$\begin{array}{rcl} \operatorname{grad} g_A(\mathbf{r}_{P_A}) & = & \lambda \cdot \operatorname{grad} g_B(\mathbf{r}_{P_B}), \\ \mathbf{r}_{P_A} - \mathbf{r}_{P_B} & = & \mu \cdot \operatorname{grad} g_B(\mathbf{r}_{P_B}), \\ g_A(\mathbf{r}_{P_A}) & = & 0, \\ g_B(\mathbf{r}_{P_B}) & = & 0. \end{array} \tag{1}$$

defining the coordinates x_{P_A}, y_{P_A}, z_{P_A}, x_{P_B}, y_{P_B}, z_{P_B} of the outer surfaces opposing points P_A, P_B, see Figure 1. Here the coordinate vectors $\mathbf{r}_{P_A} = (x_{P_A}, y_{P_A}, z_{P_A})^T$, $\mathbf{r}_{P_B} = (x_{P_B}, y_{P_B}, z_{P_B})^T$ are defined with respect to (w. r. t.) the absolute coordinate frame $O_0x_0y_0z_0$ of reference (AF) usually connected to the multibody system base body B_0. Note the functions $g_A(\mathbf{r}_0) = g_A(\mathbf{r}_0, t)$, $g_B(\mathbf{r}_0) = g_B(\mathbf{r}_0, t)$ are really a time dependent ones, and define the outer surfaces current spatial position of the bodies at a contact w. r. t. AF. The values λ, μ are an auxiliary variables.

It turned out by the computational practice with Dymola the most suitable approach to implement a system of algebraic equations like (1) is to replace it by the system of DAEs properly derived from (1). It can be done by introducing an additional variables which the time derivatives and thus compose the differential subsystem

$$\dot{\mathbf{r}}_{P_A} = \mathbf{u}_{P_A}, \quad \dot{\mathbf{r}}_{P_B} = \mathbf{u}_{P_B}, \quad \dot{\lambda} = \xi, \quad \dot{\mu} = \eta, \tag{2}$$

completed by the algebraic one

$$\begin{array}{rl} [\boldsymbol{\omega}_A, \operatorname{grad} g_A] + T_A \operatorname{Hess} f_A T_A^T (\mathbf{u}_{P_A} - \mathbf{v}_{P_A}) - & \\ \xi \operatorname{grad} g_B - & \\ \lambda([\boldsymbol{\omega}_B, \operatorname{grad} g_B] + T_B \operatorname{Hess} f_B T_B^* (\mathbf{u}_{P_B} - \mathbf{v}_{P_B})) & = \mathbf{0}, \\ \mathbf{u}_{P_A} - \mathbf{u}_{P_B} - \eta \operatorname{grad} g_B - & \\ \mu\left([\boldsymbol{\omega}_B, \operatorname{grad} g_B] + T_B \operatorname{Hess} f_B T_B^T (\mathbf{u}_{P_B} - \mathbf{v}_{P_B})\right) & = \mathbf{0}, \\ (\operatorname{grad} g_A, \mathbf{u}_{P_A}) - \left(\operatorname{grad} f_A, T_A^T \mathbf{v}_{P_A}\right) & = 0, \\ (\operatorname{grad} g_B, \mathbf{u}_{P_B}) - \left(\operatorname{grad} f_B, T_B^T \mathbf{v}_{P_B}\right) & = 0. \end{array} \tag{3}$$

where the vectors $\mathbf{v}_{P_A}$, $\mathbf{v}_{P_B}$ are a velocities of the bodies physical points currently located at the geometric points P_A, P_A and are to be calculated according to the Euler formula

$$\mathbf{v}_{P_\alpha} = \mathbf{v}_{O_\alpha} + [\boldsymbol{\omega}_\alpha, \mathbf{r}_{P_\alpha} - \mathbf{r}_{O_\alpha}] \quad (\alpha = A, B),$$

where O_A, O_B are the bodies masscenters, $\boldsymbol{\omega}_A$, $\boldsymbol{\omega}_B$ are the angular velocities of the bodies. Matrices Hess f_A, Hess f_B are the Hesse ones of the functions f_A, f_B defining the bodies outer surfaces w. r. t. the bodies central principal coordinate systems. The the functions f_A, f_B relate to the ones g_A, g_B according to the equations

$$g_\alpha(\mathbf{r}_0) = f_\alpha\left[T_\alpha^T(\mathbf{r}_0 - \mathbf{r}_{O_\alpha})\right] \quad (\alpha = A, B),$$

and their gradients connected by

$$\operatorname{grad} g_\alpha(\mathbf{r}_{P_\alpha}) = T_\alpha \operatorname{grad} f_\alpha\left[T_\alpha^T(\mathbf{r}_{P_\alpha} - \mathbf{r}_{O_\alpha})\right],$$

where T_A, T_B are the orthogonal matrices defining current orientation of the bodies.

Surely, in case of the DAEs use one has to provide a consistent initial values for all the additional state variables introduced here for each object of the compliant contact being under construction in the sequel.

Unlike our previous approach [6] now we suppose the bodies A and B don't create any obstacles for their relative motion. If 3D-regions bounded by the bodies outer surfaces don't intersect then the object of a constraint, rather of a contact, generates a zero wrench in the direction of each body. Simultaneously this object has to generate the radius vectors $\mathbf{r}_{P_A}$, $\mathbf{r}_{P_B}$ of opposing with each other points P_A, P_B.

Based on (1) note the variable μ indicates the contact of the bodies A and B. Indeed, for definiteness suppose the outer surfaces in vicinities of the points P_A, P_B are such that vectors of gradients $\operatorname{grad} g_A(\mathbf{r})$, $\operatorname{grad} g_B(\mathbf{r})$ are directed outside the each body. Then we have the following cases at hand: (a) $\mu > 0$ means the contact absent; (b) $\mu \le 0$: the contact takes place. If $\mu < 0$ then the bodies supposed to penetrate each other, though really begin to deform in a region of the contact. In the sequel we follow the simplest elastic contact model originating from Hertz [2]. Computational analysis will be performed for the case of contacting only, see Figure 2. For simplicity and definiteness the surfaces are showed convex in Figure 2 though it is not necessary at all in general for our implementation.

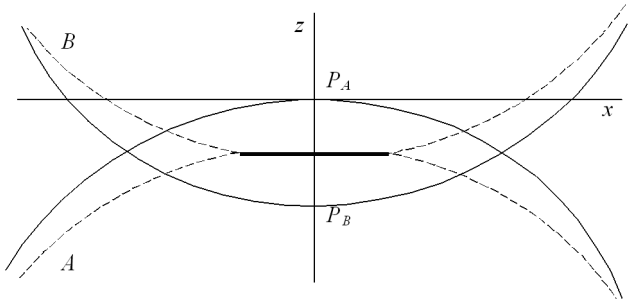

Figure 2: Local Coordinate System

To represent the Hertz contact model in its classical form first of all we have to construct an auxiliary base in vicinity of the contact. First base is composed by three unit vectors $\boldsymbol{\alpha}$, $\boldsymbol{\beta}$, $\boldsymbol{\gamma}$ such that $\boldsymbol{\gamma} = \mathbf{n}_A$, where $\mathbf{n}_A$ is the unit vector along the gradient $\operatorname{grad} g_A(\mathbf{r})$ collinear to the z-axis in Figure 2. As it was for the derivation of the opposing points the most appropriate move to compute the proper base $\{\boldsymbol{\alpha}, \boldsymbol{\beta}, \boldsymbol{\gamma}\}$ is to construct a relevant

subsystem of DAEs. First of all start with differential equation for $\boldsymbol{\gamma}$. It has the form

$$\dot{\boldsymbol{\gamma}} = |\mathrm{grad}\, g_A|^{-1} \left[(\mathrm{grad}\, g_A)^{\cdot} - (\mathbf{n}_A, (\mathrm{grad}\, g_A)^{\cdot})\, \mathbf{n}_A \right],$$

where the time derivative of the gradient reads

$$(\mathrm{grad}\, g_A)^{\cdot} = [\boldsymbol{\omega}_A, \mathrm{grad}\, g_A] + T_A \,\mathrm{Hess}\, f_A T_A^T \left(\mathbf{u}_{P_A} - \mathbf{v}_{P_A}\right).$$

Now we can right down the chain of equations

$$\boldsymbol{\Omega} = [\boldsymbol{\gamma}, \dot{\boldsymbol{\gamma}}], \quad \dot{\boldsymbol{\alpha}} = [\boldsymbol{\Omega}, \boldsymbol{\alpha}], \quad \boldsymbol{\beta} = [\boldsymbol{\gamma}, \boldsymbol{\alpha}],$$

defining successively the angular velocity $\boldsymbol{\Omega}$ of the unit vector $\boldsymbol{\gamma}(t)$ rotation, the differential equation for the unit vector $\boldsymbol{\alpha}$, and the unit vector $\boldsymbol{\beta}$ completing the local base under construction. Actually the vector $\boldsymbol{\Omega}$ is an angular velocity of the base triple $\{\boldsymbol{\alpha}, \boldsymbol{\beta}, \boldsymbol{\gamma}\}$ w. r. t. AF.

Note once more we have to provide the consistent initial data for the vectors $\boldsymbol{\alpha}$, $\boldsymbol{\gamma}$ which became now a vector valued state variables. And of course browsing the equations represented above it is transparent enough which Modelica code stands behind the algorithm outlined here.

Using the base $\{\boldsymbol{\alpha}, \boldsymbol{\beta}, \boldsymbol{\gamma}\}$ built up above it is easy enough to compose the matrix $T = [\boldsymbol{\alpha}, \boldsymbol{\beta}, \boldsymbol{\gamma}]$ consisting of the columns composed themselves by the coordinates of the unit vectors. Actually T is the transfer matrix between coordinates of AF and the current local base $\{\boldsymbol{\alpha}, \boldsymbol{\beta}, \boldsymbol{\gamma}\}$. Let us first express the outer surfaces equations in coordinates of the local system (LF) having an origin at the point P_A, see Figure 2.

Because the matrix T is orthogonal its inverse is derived by the transposition of T. Then to compute the matrix of coordinate transformation from the LF to one of the bodies' we can represent it as follows

$$R_\alpha = T^T T_\alpha \quad (\alpha = A, B).$$

Introducing new temporary notation $\mathbf{r} = (x, y, z)^T$ for the coordinate vector of the current geometric point w. r. t. local system $P_A xyz$ one can easily deduce the dependence

$$\mathbf{r} = \boldsymbol{\rho}_{O_\alpha} + R_\alpha \mathbf{r}_\alpha \quad (\alpha = A, B),$$

where $\boldsymbol{\rho}_{O_\alpha} = (\xi_{O_\alpha}, \eta_{O_\alpha}, \zeta_{O_\alpha})^T$ is the coordinate vector of the body α mass center w. r. t. LF.

Let the body α outer surface is defined by the equation

$$h_\alpha(\mathbf{r}) = 0 \quad (\alpha = A, B), \tag{4}$$

w. r. t. current position of LF. Then it is easy to see the function h_α can be computed by the formula

$$h_\alpha(\mathbf{r}) = f_\alpha\left(R_\alpha^T\left(\mathbf{r} - \boldsymbol{\rho}_{O_\alpha}\right)\right) \quad (\alpha = A, B).$$

Further bring the equations (4) to the form suitable to analyse the contact problem in vicinity of the corresponding points

$$\boldsymbol{\rho}_{P_\alpha} = \boldsymbol{\rho}_{O_\alpha} + R_\alpha \boldsymbol{\rho}_\alpha \quad (\alpha = A, B),$$

on the surface of the body α. Here the vector $\boldsymbol{\rho}_\alpha$ defines the position of the point P_A w. r. t. the body α own coordinate system. Supposing the surfaces regular enough we have the expansions

$$\begin{aligned} f_\alpha(\mathbf{r}_\alpha) &= f_\alpha(\boldsymbol{\rho}_\alpha) + (\mathrm{grad}\, f_\alpha(\boldsymbol{\rho}_\alpha), \Delta\mathbf{r}_\alpha) + \\ &\quad \frac{1}{2}\left(\mathrm{Hess}\, f_\alpha(\boldsymbol{\rho}_\alpha)\Delta\mathbf{r}_\alpha, \Delta\mathbf{r}_\alpha\right) + O\left(|\Delta\mathbf{r}_\alpha|^3\right), \\ h_\alpha(\mathbf{r}) &= h_\alpha\left(\boldsymbol{\rho}_{P_\alpha}\right) + \left(\mathrm{grad} h_\alpha\left(\boldsymbol{\rho}_{P_\alpha}\right), \Delta\mathbf{r}\right) + \\ &\quad \frac{1}{2}\left(\mathrm{Hess} h_\alpha\left(\boldsymbol{\rho}_{P_\alpha}\right)\Delta\mathbf{r}, \Delta\mathbf{r}\right) + O\left(|\Delta\mathbf{r}|^3\right), \end{aligned}$$

where $\Delta\mathbf{r} = \mathbf{r} - \boldsymbol{\rho}_{P_\alpha}$, $\Delta\mathbf{r}_\alpha = \mathbf{r}_\alpha - \boldsymbol{\rho}_\alpha$. Since $\Delta\mathbf{r} = R_\alpha \Delta\mathbf{r}_\alpha$ then it is easy to verify that

$$\begin{aligned} \mathrm{grad} h_\alpha\left(\boldsymbol{\rho}_{P_\alpha}\right) &= R_\alpha \mathrm{grad}\, f_\alpha(\boldsymbol{\rho}_\alpha) \\ \mathrm{Hess} h_\alpha\left(\boldsymbol{\rho}_{P_\alpha}\right) &= R_\alpha \mathrm{Hess}\, f_\alpha(\boldsymbol{\rho}_\alpha) R_\alpha^T. \end{aligned} \tag{5}$$

Because at the body α outer surface point $\boldsymbol{\rho}_{P_\alpha}$ the function h_α is zero-valued then up to the terms of the third order in the coordinate system $P_\alpha xyz$ the equation (4) can be represented as follows

$$\frac{\partial h_\alpha}{\partial z} z + \begin{pmatrix} x & y \end{pmatrix} \begin{pmatrix} a_\alpha & c_\alpha \\ c_\alpha & b_\alpha \end{pmatrix} \begin{pmatrix} x \\ y \end{pmatrix} = 0, \tag{6}$$

where the Hesse matrix elements are to be expressed by the formulae

$$a_\alpha = \frac{1}{2}\frac{\partial^2 h_\alpha}{\partial x^2}, \quad b_\alpha = \frac{1}{2}\frac{\partial^2 h_\alpha}{\partial y^2}, \quad c_\alpha = \frac{1}{2}\frac{\partial^2 h_\alpha}{\partial x \partial y},$$

where in turn one should use the results of (5). Note the equation (6) has such a simple representation because at the point $\boldsymbol{\rho}_{P_\alpha}$ the choice of the base causes the conditions

$$\frac{\partial h_\alpha}{\partial x}\left(\boldsymbol{\rho}_{P_\alpha}\right) = 0, \quad \frac{\partial h_\alpha}{\partial y}\left(\boldsymbol{\rho}_{P_\alpha}\right) = 0. \tag{7}$$

Supposing the surfaces are nondegenerate at the points P_α we have the condition

$$|\mathrm{grad} h_\alpha(\mathbf{r}_\alpha)| > 0,$$

and because of (7) it causes the condition

$$\frac{\partial h_\alpha}{\partial z}(\mathbf{r}_\alpha) \neq 0.$$

Therefore, the equation (6) can be resolved w. r. t. the variable z in explicit form as

$$z = a'_\alpha x^2 + 2c'_\alpha xy + b'_\alpha y^2, \tag{8}$$

where the new coefficients of the second order terms are computed in the form

$$a'_\alpha = -\frac{a_\alpha}{\frac{\partial h_\alpha}{\partial z}}, \quad b'_\alpha = -\frac{b_\alpha}{\frac{\partial h_\alpha}{\partial z}}, \quad c'_\alpha = -\frac{c_\alpha}{\frac{\partial h_\alpha}{\partial z}}.$$

The further reduction comes to a transformation to canonical view of the quadratic form

$$q(x,y) = ax^2 + 2cxy + by^2, \tag{9}$$

derived as a difference between the forms (8) such that

$$a = a'_B - a'_A, \quad b = b'_B - b'_A, \quad c = c'_B - c'_A.$$

The transformation is implemented simply as a rotation about the z-axis of the system $P_A xy$ to achieve the coefficient c vanishes. Finally the function (9) becomes having the form

$$q(x,y) = Px^2 + Qy^2 \tag{10}$$

with the additional condition $0 < P \leq Q$.

3 The Hertz Model

According to the known technique [7] to compute the total normal force at the contact we have to solve the system

$$\begin{aligned} \frac{FD}{\pi}\int_0^\infty \frac{d\xi}{\sqrt{(\alpha+\xi)(\beta+\xi)\xi}} &= h, \\ \frac{FD}{\pi}\int_0^\infty \frac{d\xi}{(\alpha+\xi)\sqrt{(\alpha+\xi)(\beta+\xi)\xi}} &= P, \\ \frac{FD}{\pi}\int_0^\infty \frac{d\xi}{(\beta+\xi)\sqrt{(\alpha+\xi)(\beta+\xi)\xi}} &= Q, \end{aligned} \tag{11}$$

of three transcendental equations provided the coefficients P, Q from the representation (10) and depth of mutual penetration, so-called mutual approach, $h = |\mathbf{r}_{P_B} - \mathbf{r}_{P_A}|$ are already have been computed. The system (11) has three unknown variables: α, β, F, where the values α, β are the semi-major axes squared of the contact spot ellipse, and F is the total normal elastic force really distributed over the contact area. The parameter

$$D = \frac{3}{4}\left(\frac{1-\nu_A^2}{E_A} + \frac{1-\nu_B^2}{E_B}\right)$$

summarizes elastic properties of the contacting bodies: ν_A, ν_B being Poisson's ratios, and E_A, E_B being corresponding Young's moduli.

Using the substitution $\xi \mapsto \eta$ ($\xi = \lambda\eta$) in elliptic integrals of (11) we can separate the last two equations of (11). Indeed, introducing new scaled unknown variables α', β' according to formulae $\alpha' = \alpha/\lambda$, $\beta' = \beta/\lambda$ we can deduce the two mentioned equations to the closed system

$$I_1(\alpha',\beta') = P, \quad I_1(\beta',\alpha') = Q, \tag{12}$$

if the scaling factor λ satisfies the norming condition

$$\frac{FD}{\pi}\cdot\frac{1}{\lambda^{3/2}} = 1. \tag{13}$$

Here the elliptic integral $I_1(\alpha,\beta)$ is defined by

$$I_1(\alpha,\beta) = \int_0^\infty \frac{d\xi}{(\alpha+\xi)\sqrt{(\alpha+\xi)(\beta+\xi)\xi}}$$

causing clearly verified equations

$$I_1(\alpha',\beta') = -2\frac{\partial I(\alpha',\beta')}{\partial\alpha'}, \; I_1(\beta',\alpha') = -2\frac{\partial I(\alpha',\beta')}{\partial\beta'}, \tag{14}$$

where taking into account that $\alpha' \geq \beta'$, which is equivalent to the condition $P \leq Q$ satisfied above, we may have the relations

$$I(\alpha',\beta') = \int_0^\infty \frac{d\xi}{\sqrt{(\alpha'+\xi)(\beta'+\xi)\xi}} = \frac{2}{\sqrt{\alpha'}}\mathsf{K}(k),$$

where in turn $\mathsf{K}(k)$ is the complete elliptic integral of the first kind with the modulus defined by the formula

$$k = \sqrt{\frac{\alpha'-\beta'}{\alpha'}}.$$

Here one can see the value k actually has a geometric sense exactly of the contact spot ellipse eccentricity. Using the work [8] as a pattern we introduce the value $c = k^2$ of the elliptic integral modulus square. Taking into account that elliptic integrals are regular functions of $c = 1-\beta'/\alpha'$ we obtain using the rule of the compound function differentiation

$$\begin{aligned} I_1(\alpha',\beta') &= \frac{2}{\alpha'^{3/2}}\left(\mathsf{K}(c) - 2(1-c)\frac{d\mathsf{K}(c)}{dc}\right), \\ I_1(\beta',\alpha') &= \frac{4}{\alpha'^{3/2}}\frac{d\mathsf{K}(c)}{dc}. \end{aligned}$$

Dividing then the first equation of (12) by the second one and using the last derived expressions we reduce finally the whole problem to the one-dimensional transcendental equation

$$\frac{1}{2}\mathsf{K}(c)\left(\frac{d\mathsf{K}(c)}{dc}\right)^{-1} - (1-c) = \frac{P}{Q} \tag{15}$$

w. r. t. the unknown value c.
Once the solution of the equation (15) had been found we can obtain immediately the values

$$\alpha' = \left(\frac{4}{Q}\frac{d\mathsf{K}(c)}{dc}\right)^{2/3} \quad \beta' = \alpha'(1-c).$$

Using the first equation of (11) and normalizing dependence (13) we then find the value of the scaling factor

$$\lambda = \frac{h}{I(\alpha',\beta')} \tag{16}$$

thus arriving to the Hertz problem solution: the normal force and the contact ellipse semi-major axes values

$$F = \frac{\pi}{D}\lambda\sqrt{\lambda}, \quad a = \sqrt{\lambda\alpha'}, \quad b = \sqrt{\lambda\beta'}.$$

Nevertheless an implementation on Dymola requires a further reduction of the model in a manner we already mentioned above twice: use preferably the differential equations (probably to overcome the potential problems for the analytical processor when differentiating the transcendental expressions on the DAE system index reduction stage when compiling and indirectly and more rarely when running the model). To this end we have to remind the known ODEs connecting the complete elliptic integrals of the first $\mathsf{K}(c)$ and the second $\mathsf{E}(c)$ kind between one another [8]

$$\frac{d\mathsf{K}}{dc} = \frac{\mathsf{E}-(1-c)\mathsf{K}}{2c(1-c)}, \quad \frac{d\mathsf{E}}{dc} = \frac{\mathsf{E}-\mathsf{K}}{2c}.$$

Furthermore instead of (15) then we should use its differential version

$$\left[3\left(\frac{d\mathsf{K}}{dc}\right)^2 - \mathsf{K}\frac{d^2\mathsf{K}}{dc^2}\right]\dot{c} = 2\left(\frac{d\mathsf{K}}{dc}\right)^2\dot{C},$$

where $C = P/Q$, and

$$\frac{d^2\mathsf{K}}{dc^2} = \frac{(1-c)(2-3c)\mathsf{K}-(2-4c)\mathsf{E}}{4c^2(1-c)^2}.$$

In this way the complete integrals become an additional state variables such that

$$\dot{\mathsf{K}} = \frac{d\mathsf{K}}{dc}\dot{c}, \quad \dot{\mathsf{E}} = \frac{d\mathsf{E}}{dc}\dot{c},$$

and simultaneously we have yet another way to compute elliptic integrals in dynamics, note: exclusively fast and sufficiently accurate way.
Staying in frame of the traditional Hertz model and taking into account that the expression for the normal force has the form

$$F_{\text{elast}} = -e(P,Q)h^{3/2},$$

where while changing the value h the values P, Q don't change, we conclude the potential energy of elastic deformations is represented by the expression

$$U_{\text{elast}} = \frac{2}{5}e(P,Q)h^{5/2}.$$

On the other hand using the volumetric approach [5] one can try to represent the same potential energy as follows

$$U_{\text{elast}} = f\left(\frac{b}{a}\right)V^{\nu}S^{\sigma}p^{\delta},$$

where V is the volume of the bodies undeformed material intersected, S is the area of the intersection projection onto the xy-plane of the LF, p is the perimeter of that projection. It turned out if $\nu = 2$, $\sigma = -7/4$, $\delta = 1/2$ then the function

$$V_{\text{elast}} = 0.357469\frac{8}{15\pi^{1/4}(\theta_A+\theta_B)}\frac{V^2p^{1/2}}{S^{7/4}},$$

differs from U_{elast} by 0.5% of its value in wide range of the contact ellipse shapes: surely for $b/a \in [0.1,1]$. Here

$$\theta_\alpha = \frac{1-\nu_\alpha^2}{\pi E_\alpha}, \quad (\alpha = A,B).$$

Since in the case of the Hertz model the contact spot is the ellipse then the values V, S, p are to be computed by the expressions

$$V = \frac{\pi h^2}{2\sqrt{PQ}}, \; S = \frac{\pi h}{2\sqrt{PQ}}, \; p = \frac{4\sqrt{h}(Q/P)^{1/4}\mathsf{E}(c_1)}{(PQ)^{1/4}},$$

where the elliptic integral modulus squared this time has the expression $c_1 = 1 - P/Q$. Then taking into account that

$$F_{\text{elast}} = -\frac{\partial U_{\text{elast}}}{\partial h},$$

we get the Vilke formula for the approximate value of the normal force at the contact

$$F_{\text{elast}} = -0.357469\frac{2}{3(\theta_A+\theta_B)}\frac{\sqrt{\mathsf{E}(c_1)}}{P^{3/8}Q^{3/8}}h^{3/2}.$$

Numeric experimental verification showed an application of the above expression for the normal force indeed causes the relative error near the value 0.5% for the contacting bodies configuration coordinates in compare with "exact" Hertz model over long time of simulation. Anyway to estimate with the proper quality the fatigue processes in machines while the lifecycle simulation it is sufficient enough to have an acceptable approximation for the contact forces.
The Vilke formula is essentially simpler than computations in the Hertz model requiring the solution of the

transcendental equation. Volumetric derived algorithm is more reliable than the Hertz one though sometimes due to the differential techniques arranged for the elliptic integrals the Hertz algorithm works even faster than one of Vilke.

4 Implementation

The procedures described above to compute the normal force of an elastic interaction were implemented on Modelica in frame of general approach to construct the objects of mechanical constraint [9]. Strictly speaking in case of the compliant connection the constraint itself is absent. Instead we have an elastic compliance implementing the Hertz contact model. Though the general architecture of the objects interaction conserves completely. Thus for future purpose retain the term "constraint".

When implementing a class of the compliant interaction it turned out to be useful to split its base classes in two different lines of inheritance: (a) the first one contains mainly the geometric properties, (b) the second line is responsible for the normal force calculation. Thus in the last derived class we use the multiple inheritance allowed in Modelica. An example of the classes hierarchy in the case under consideration see in Figure 3.

The example is one of the simplest ones to test an implementation of the Hertz model: the contact of the ellipsoid and the plane. The left line of inheritance, see Figure 3, concerning mainly with the contact geometric properties

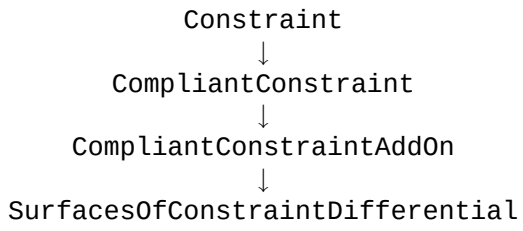

has a common use and doesn't depend on the type of the contacting surfaces. The variables which do depend on such that gradients and the Hesse matrices are evaluated in the class

`EllipsoidAndHorizontalPlaneDifferential`.

The class `SurfacesOfConstraintDifferential` is here the most essential derived one. It is responsible for the points P_A and P_B permanent tracking, implements the DAE system (2), (3), and has the following Modelica code

```
partial model
  SurfacesOfConstraintDifferential
  extends CompliantConstraintAddOn;
  SI.Velocity[3] drA;
  SI.Velocity[3] drB;
  ConstraintDetectorRate dmu;
  Real lambda;
  LambdaRate dlambda;
  GradientRate[3] dgradgA;
  GradientRate[3] dgradgB;
  Real Active(start = 1);
  Hessian[3, 3] HessgA;
  Hessian[3, 3] HessgB;
equation
  der(Active) = 0;
  der(rA) = Active*drA;
  der(rB) = Active*drB;
  der(lambda) = Active*dlambda;
  der(mu) = Active*dmu;
  dgradgA = cross(InPortA.omega, gradgA)
    + HessgA*(drA - vrA);
  dgradgB = cross(InPortB.omega, gradgB)
    + HessgB*(drB - vrB);
  dgradgA = lambda*dgradgB +
    dlambda*gradgB;
  drA - drB = mu*dgradgB + dmu*gradgB;
  0 = gradgA*(drA - vrA);
  0 = gradgB*(drB - vrB);
  HessgA = InPortA.T*HessfA*
    transpose(InPortA.T);
  HessgB = InPortB.T*HessfB*
    transpose(InPortB.T);
end SurfacesOfConstraintDifferential;
```

where the variables correspond to ones in (2), (3) in an evident way by use of their names.

In the line of the force properties inheritance

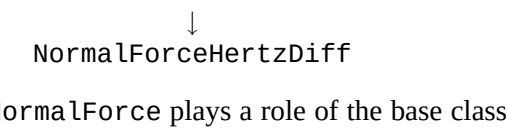

the class `NormalForce` plays a role of the base class for any implementation of the normal force. In the class `NormalForceHertzDiff` the normal force besides the elastic Hertzian term has the term of viscosity of the form

$$F_{\text{visc}} = -d(h)\dot{h},$$

where h is the mutual approach. This latter term supposed to arise due to the plasticity properties of the material the bodies made of. It is fair natural to consider the coefficient at $\dot{h}$ to depend upon h [10] since as the mutual approach increases from zero then the contact spot area also increases from zero. Therefore it is quite natural for the plastic resistance to increase continuously from zero.

The class `NormalForceHertzDiff` Modelica code is long enough thus let us highlight some of its main features, namely the implementation of the auxiliary

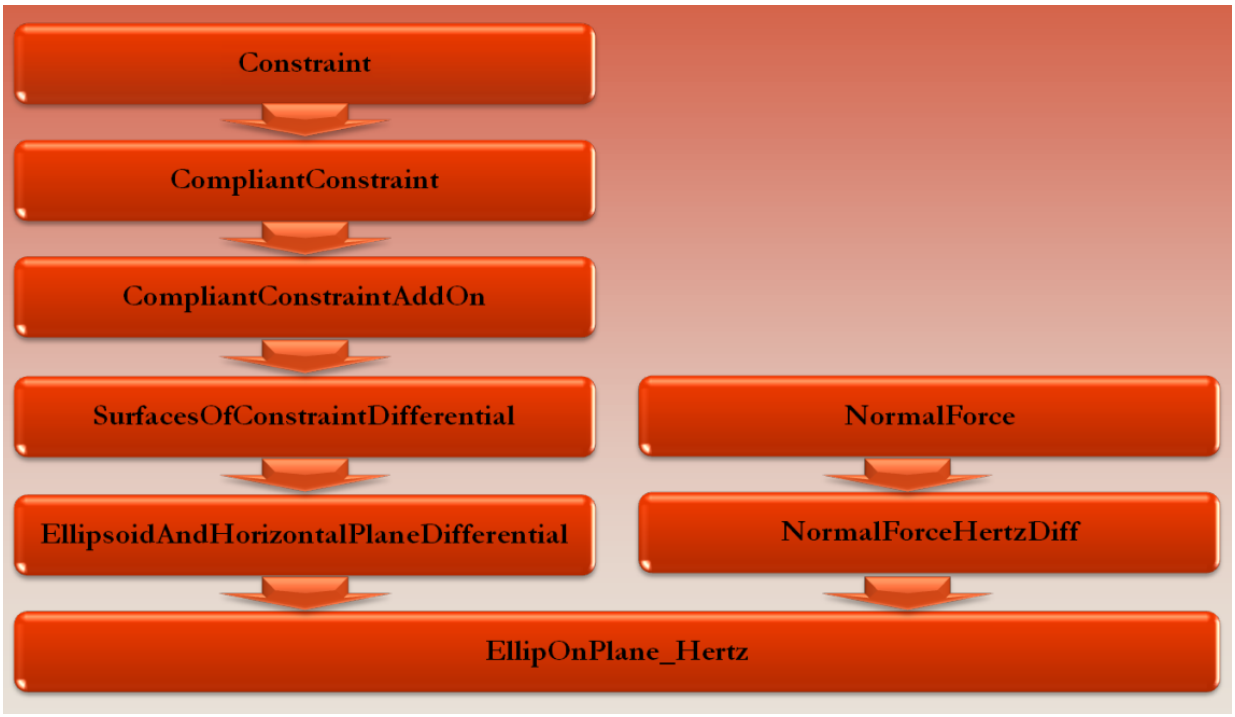

Figure 3: Example of Compliant Constraint Classes Hierarchy

local base $\{\boldsymbol{\alpha}, \boldsymbol{\beta}, \boldsymbol{\gamma}\}$ tracking and equations to compute the solution of the system of the transcendental equations

```
model NormalForceHertzDiff
  ...
initial equation
  K = CompleteEllOfFirstKind(k2);
  E = CompleteEllOfSecondKind(k2);
  0.5*CompleteEllOfFirstKind(k2)/
    dKdk2(k2) - (1 - k2) = C;
equation
  dgamma = (dgradgA1 -
    normA1*(normA1*dgradgA1))
    /sqrt(gradgA1*gradgA1);
  der(gamma) = dgamma;
  OmegaA = cross(gamma, dgamma);
  der(alpha) = cross(OmegaA, alpha);
  beta = cross(gamma, alpha);
  ...
  der(k2) = dk2;
  dK = if k2 < Accuracy then dKdk2(k2)
    else 0.5*(E - (1 - k2)*K)/k2
    /(1 - k2);
  dE = if k2 < Accuracy then dEdk2(k2)
    else 0.5*(E - K)/k2;
  der(K) = dK*dk2;
  der(E) = dE*dk2;
  C = A1/B1;
  dC = der(C);
  ddK = if k2 < Accuracy then
    d2Kdk22(k2) else 0.25*((1 - k2)*
    (2 - 3*k2)*K - (2 - 4*k2)*E)/k2^2
    /(1 - k2)^2;
  (3*dK^2 - K*ddK)*dk2 = 2*dK^2*dC;
  ...
end NormalForceHertzDiff;
```

where the variables K, E, k2, dK, dE, ddK, A1, B1, C stand correspondingly for the values $\mathsf{K}(c)$, $\mathsf{E}(c)$, c, $d\mathsf{K}/dc$, $d\mathsf{E}/dc$, $d^2\mathsf{K}/dc^2$, P, Q, C from previous section. The functions dKdk2(k2), dEdk2(k2), d2Kdk22(k2) are used if the modulus is small enough, i. e. regular expressions become inoperative. These functions are computed via expansions of series with the fast convergence for the small modulus. Section of initial equations is needed to initialize a state variables being computed using known expansions for the complete elliptic integrals. These expansions work only once when starting the simulation.

A tangent force at the contact in our case is computed in the class CompliantConstraintAddOn and for the simplicity is implemented as a regularized model of the Coulomb friction [6]. Obviously, one can create here even far more complicated models for the tangent force at the contact.

5 Example of the Ball Bearing

The ball bearing model is built up using the architectural principle mentioned above. On the Icon-level of its representation it looks exactly like the model

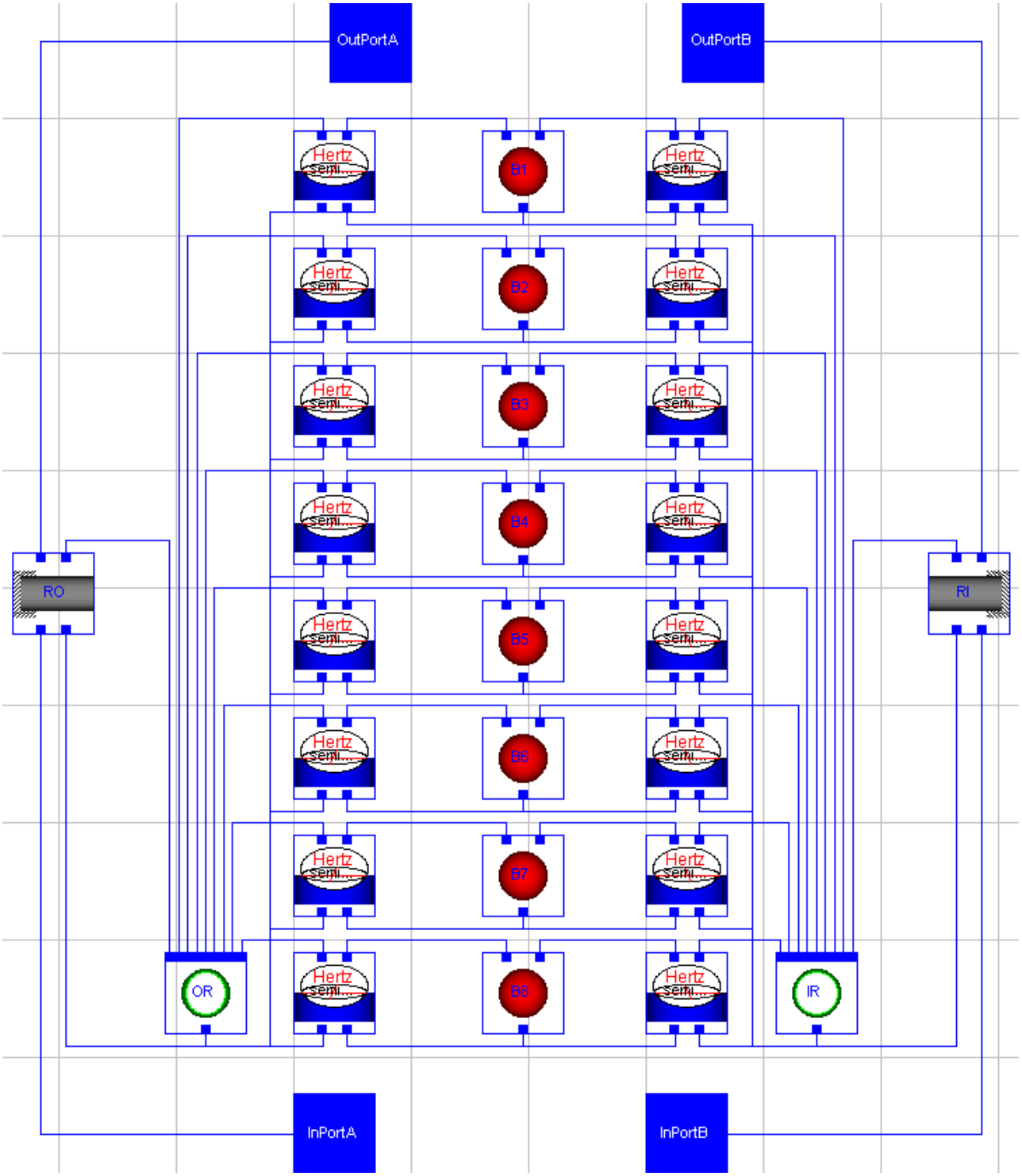

Figure 4: Visual Model of the Ball Bearing

of any constraint: it has two ports of the connector type `KinematicPort` to import the twists of the rigid bodies connected by the bearing, and two ports of the `WrenchPort` type to export the wrenches in directions of the bodies mentioned. Visual model of the ball bearing see in Figure 4

For definiteness the bearing was equipped by eight balls. Each ball has two elastic contacts: one with the inner ring, and one with the outer one. In both cases when contacting the ball simultaneously rolls over the surfaces of the toroidal tubes corresponding to the raceways of the inner and outer rings.

Describe in brief the specifications of the contact between the ball and one of the toroidal raceways. The ring always supposed to be denoted as a body A in the contact object of the ball bearing model, while the ball always denoted as B. All we need to complete the constraint specifications is to define the functions f_A, f_B. In our case we have

$$\begin{aligned} f_A(x,y,z) &= 4R_A^2\left(x^2+y^2\right) - \\ &\quad \left(x^2+y^2+z^2+R_A^2-r_A^2\right)^2, \\ f_B(x,y,z) &= x^2+y^2+z^2-R_B^2, \end{aligned}$$

where r_A is the toroidal pipe radius, R_A is the radius of the circle being an axis of that toroidal pipe, R_B is the ball radius.

Paying an attention to the ball bearing visual model, Figure 4, note the central column represents eight objects `B1`, `B2`, ..., `B8` of elastic balls. Left and right columns of objects composed by the contact objects between the balls and the outer ring (left column) and inner ring (right column), all implemented using the Hertz model described above. The objects representing in the model the inner and outer rings have the names `IR` and `OR` correspondingly. At left and right extreme sides of the class the objects of rigid constraints are located. These constraints connect the outer and the inner rings objects with the objects of the bodies, outer and inner shafts in our case, attached one with another by the bearing. In the example under consideration the body connected with the outer ring rests w. r. t. AF while the body connected to the inner ring rotates uniformly about z-axis of AF both thus performing the prescribed motion, see the animation image in Figure 5.

The visual model of the example testbench see in Figure 6. To verify the quality of the Hertz model implementation we compared the vectors $\boldsymbol{\gamma}$ and $\mathbf{n}_A$ as functions of time. The computational experiments showed that their coordinates coincide with a very high accuracy. At last yet another remark: to make the simulation even more faster, at least twice, one can apply the

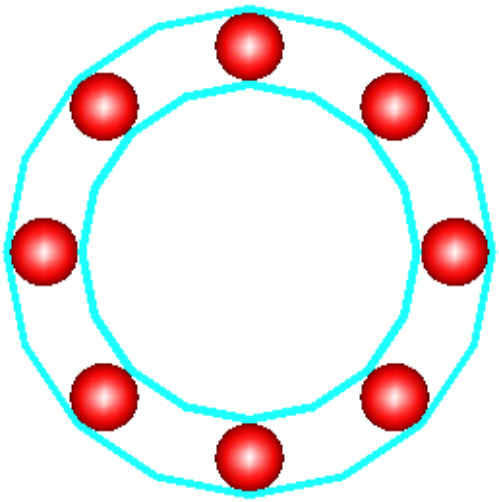

Figure 5: Animation of the Model

simplified expression of the form

$$F_{\text{elast}} = -eh^{3/2},$$

with the constant coefficient e for the normal elastic force at the contact [11]. But it is possible only if the geometric properties (curvatures etc.) don't change while simulating the model. Moreover, for different cases of contacting the coefficient e would have different values. Then its value can be computed using the numerical experiment, or even better using the natural physical experiment. If the motion under simulation is perturbed from its pure case with the constant e then immediately its value begins change in time.

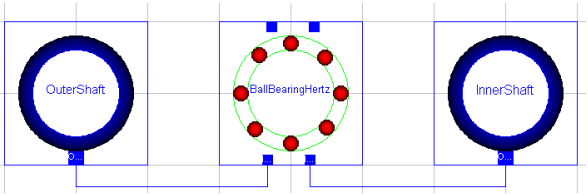

Figure 6: Visual Model of the Testbench

6 Conclusions

Summarizing the results presented above we can split them to the several main remarks influencing the potential directions of future work:

(1) According to an experience accumulated while developing the models simulating the multibody dynamics one can resume the usefulness of the approach when the differential formulations proper applied are preferable in several aspects. It is a real way to han-

dle the transcendental equations in frame of dynamical problems using the ODEs derived from the transcendental ones in combination with the linear solver w. r. t. derivatives of the new state variables.
(2) In particular it turned out an introduction of the component of the ODEs system for the elastic bodies outer surfaces tracking for the contact problem conserves an accuracy and simultaneously improves the reliability of the models. To implement the tracking in case of the complex shape surfaces we have to rearrange only one derived class at the end of the inheritance chain to define an equations for the gradients and Hessians of the surfaces A and B w. r. t. LFs of the bodies. The surfaces supposed smooth enough and without sharp edges but can be described by `if`-constructs properly arranged.
(3) Implementation of the complete elliptic integrals using ODEs subsystem also was useful: the models became more reliable and faster. For instance, the Hertz algorithm improved as described above turned out to be even faster than the V. G. Vilke one in case of the almost circular contact area.
(4) The algorithm of V. G. Vilke is more reliable and suitable for wide range of the contact area eccentricities simultaneously providing an accuracy of 0.5% with respect to the Hertz-point algorithm.
Regarding the directions of the future work it is evident enough an interest to apply the developed models to different types of appliances with the rotary motions, or to the problems essentially including the effects of friction when contacting.

7 Acknowledgement

The paper was prepared with partial support of Russian Foundation for Basic Research, projects 05-01-00308-a, 05-08-65470, 05-01-00454, SS-6667.2006.1.

References

[1] Gonthier Y., Lange C., McPhee J., On Implementing a Bristle Friction Model in a Contact Model Based on Volumetric Properties // Multibody Dynamics 2007, ECCOMAS Thematic Conference, Proceedings, Politecnico di Milano, Milano, Italy, June 25–28, 2007.

[2] Hertz H. Über die Berührung fester elastischer Körper // J. reine und angewandte Mathematik. B. 92. 1882. S. 156–171.

[3] Hippmann G., An Algorithm for Compliant Contact Between Complexly Shaped Bodies // Multibody System Dynamics, 2004, Vol. 12, pp. 345–362.

[4] Otter M., Elmqvist H., Lopez J. D., Collision Handling for the Modelica MultiBody Library // Proceedings of the 4th International Modelica Conference, Hamburg University of Technology, Hamburg–Harburg, Germany, March 7–8, 2005, pp. 45–53.

[5] Vilke V. G., On Non-Hertzian Contact of Wheel and Rail // Research on Problems of Stability and Stabilization of Motion. Reports of the Computing Center of the Russian Ac. of Sc., (in press).

[6] Kossenko I. I., Implementation of Unilateral Multibody Dynamics on Modelica // Proceedings of the 4th International Modelica Conference, Hamburg University of Technology, Hamburg–Harburg, Germany, March 7–8, 2005, pp. 13–23.

[7] Landau L. D., Lifshitz E. M., Theory of Elasticity. 3rd Edition. Landau and Lifshitz Course of Theoretical Physics. Volume 7. — Reed Educational and Professional Publishing Ltd.: Oxford – Boston – Johannesburg – Melbourne – New Delhi – Singapore, 1999.

[8] Whittaker E. T., Watson G. N., A Course of Modern Analysis, — Cambridge University Press: Cambridge – New York – Melbourne – Madrid – Cape Town, 2002.

[9] Kosenko I. I., Loginova M. S., Obraztsov Ya. P., Stavrovskaya M. S., Multibody Systems Dynamics: Modelica Implementation and Bond Graph Representation // Proceedings of the 5th International Modelica Conference, arsenal research, Vienna, Austria, September 4–5, 2006, pp. 213–223.

[10] Wensing J. A., On the Dynamics of Ball Bearings. PhD Thesis. — University of Twente: Enschede, The Netherlands, 1998.

[11] Lee S., Park T., Park J., Yoon J., Jeon Y., Jung S., Fatigue Life Prediction of Guideway Vehicle Components // Multibody Dynamics 2007, ECCOMAS Thematic Conference, Proceedings, Politecnico di Milano, Milano, Italy, June 25–28, 2007.